Muscle Fatigue Assessment in a Wearable Neuroprosthesis Using Ultrasound Strain Imaging

Zhiyu Sheng[1], Nitin Sharma[1, 2, 3], Kang Kim[1, 2, 4, 5]

[1] Department of Mechanical Engineering and Materials Science, University of Pittsburgh, Pittsburgh, PA, USA.
[2] Department of Bioengineering, University of Pittsburgh, Pittsburgh, PA, USA.
[3] Clinical and Translational Science Institute at the University of Pittsburgh, Pittsburgh, PA, USA.
[4] Center for Ultrasound Molecular Imaging and Therapeutics, Department of Medicine and Heart and Vascular Institute, University of Pittsburgh and University of Pittsburgh Medical Center, Pittsburgh, PA, USA
[5] McGowan Institute for Regenerative Medicine, University of Pittsburgh and University of Pittsburgh Medical Center, Pittsburgh, PA, USA.

Email: zhs41@pitt.edu, nis62@pitt.edu, kangkim@upmc.edu.

Abstract: *An ultrasound imaging-based methodology was proposed to quantify the fatigue development in a wearable neuroprosthesis using a functional electrical stimulation (FES). Force data and ultrasound images were recorded synchronously in isometric knee extension experiments on a human participant. The maximum axial strain was estimated from muscle displacement tracking results during each stimulated muscle contraction. Analysis of the strain images indicates a decreasing trend of the maximum axial strain and a monotonic trend of the strain distribution. The reduction of the maximum strain is correlated with the reduction of the maximum joint torque. The results show that ultrasound imaging with the proposed methodology is promising for being integrated into a wearable neuroprosthesis to assess the FES-induced muscle fatigue.*

Keywords: *Ultrasound imaging, functional electrical stimulation (FES), muscle fatigue*

Introduction

One of the main goals in rehabilitation of patients with spinal cord injuries (SCI) is to restore their limb functions. Neuroprosthetic devices that utilize functional electrical stimulation (FES) to recruit motor units through low energy electrical pulses have been developed to facilitate these challenges [1]–[4]. Beside a beneficial training effect on muscle, compared with powered exoskeletons which have a large battery to support electrical motors, a neuroprosthesis with FES is much less bulkier, more flexible and wearable. Nevertheless, a quick onset of muscle fatigue raises a significant challenge in FES applications [5], [6]. The effectiveness and accuracy of FES control decreases due to the fatigue and thus limits its operating duration.

Strategies for resolving loss in effectiveness relies on modeling and assessing the FES-induced fatigue development. Methodologies of measuring muscle fatigue include direct force measurement [7], electromyography (EMG) or surface electromyography (sEMG) [8]–[10], mechanomyography (MMG) [11]–[13], near-infrared spectroscopy (NIRS) [11] and phosphorus nuclear magnetic resonance (NMR) [14]. However, *in vivo* force measurement of a specific targeted muscle is non-trivial. sEMG-based methods usually target those muscles that are directly below the skin [10] and possibly get a signal interference due to cross talk among neighbouring muscles [10] or from artifacts originating from electrical stimulations [15]. MMG remains as a topic for further investigation in clinical practices [13]. NIRS and NMR currently are not easily implementable in real-time FES applications.

Alternatively, real time ultrasound imaging known for its non-invasiveness and capability of imaging muscles at a wide range of depth has been proposed as a promising sensor modality for wearable prosthetic systems [16], [17]. To specifically investigate the effect of muscle fatigue via ultrasound imaging, Witte et al. in [18] studied the 3rd flexor digitorum superficialis muscle and showed the elastic and viscoelastic-like modifications on the ultrasound strain imaging before and after a volitional fatigue exercise. Shi et al. in [19] analyzed an exercise-induced fatigue in the right biceps brachii muscle by defining a thickness change from the cross-sectional ultrasound images. In this paper, we propose an ultrasound imaging-based methodology to assess muscle contractility change during the whole transition period including pre-fatigue, peri-fatigue and post-fatigue stages. An FES stimulated isometric knee extension in a human participant was elicited. The isometric force and ultrasound image data were synchronously collected.

During the isometric knee extension, due to the fatigue caused by a constant FES input, there was a simultaneous decrease of both the muscle contraction and the maximum force produced by each contraction. We consider that a muscle contraction can be characterized by the maximum deformation of the stimulated muscle. This is further quantified by the maximum value of a strain measure derived from the ultrasound images per a muscle contraction. As a result, a potential strain-force correlation can be established. A gradual reduction of the maximum strain measure among consecutive contractions quantifies the change in muscle contractility during the development of FES induced muscle fatigue.

Methods

Axial strain from ultrasound images: Deformation of the stimulated quadriceps muscle can be estimated using a two dimensional plane strain if the muscle movement is assumed

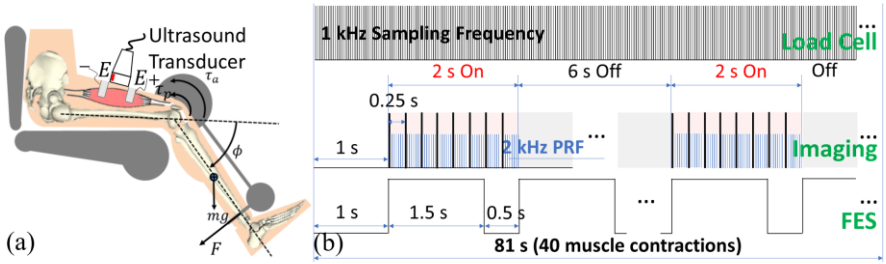

(a) A Sketch of the stimulated isometric knee extension experiment with ultrasound imaging. (b) The experiment protocol under a data synchronization scheme. Pulse repetition frequency (PRF) of the plane wave ultrasound imaging is 2 kHz.

to be limited within the imaging plane. In continuum mechanics, the deformation gradient tensor can be expressed by a diagonal matrix if there is no rotation and the principal axes of the right stretch tensor remain close to the axial and lateral directions of the ultrasound image coordinate system shown in Fig. 2g. Axial and lateral strain measures, $\varepsilon_1(x,y)$, $\varepsilon_2(x,y)$, at a position, (x,y), can then be calculated by taking the spatial derivatives of the displacement field $\vec{d}(x,y) = (d_x(x,y), d_y(x,y))$, as $\varepsilon_1(x,y) = \frac{\partial d_x(x,y)}{\partial x}$ and $\varepsilon_2(x,y) = \frac{\partial d_y(x,y)}{\partial y}$. In addition, due to soft tissue incompressibility, it is reasonable to use a single scalar field $\varepsilon_1(x,y)$, which is the axial strain, to characterize muscle contraction within the selected ultrasound imaging plane.

To estimate the displacement from consecutive ultrasound image series, of which the gradient is the defined strain measure, a modified speckle tracking algorithm based on the two dimensional normalized cross correlation [20] was applied with two steps. Firstly, appropriate image frames were selected from the images sequence and the frame to frame displacement was tracked by the algorithm. The criteria of selecting these frames is to approximate the magnitude of the displacement before tracking and maintain it in a reasonable range. More specifically, tracking should be conducted between all the consecutive frames when muscle moves very fast while skipping of several frames is preferred when muscle contracts at a relatively low speed. This not only ensures the quasi-static tracking that minimizes the speckle decorrelation, but also reduces unnecessary noise accumulation when summing the frame to frame tracking results. Secondly, the frame to frame displacement was accumulated across all the selected frames and the displacement field $\vec{d}(x,y)$ with respect to an initial reference frame was obtained.

Apparatus: The isometric knee extension was performed by stimulating the quadriceps muscle of a human participant under a fatiguing protocol while both the force and ultrasound image data were synchronously collected during the whole period. The setup was illustrated by Fig. 1a. To image the targeted quadriceps muscle in the longitudinal direction that is mostly aligned with the muscle fiber, a clinical ultrasound linear transducer (L7.5SC Prodigy Probe, S-Sharp, Taiwan) connected to the ultrasound imaging system (Prodigy, S-Sharp, Taiwan) was attached on the thigh. One of the obtained ultrasound images aimed at a region of interest (ROI), where the quadriceps muscle contracts, is shown in Fig. 2g. On the image, the left hand side is the proximal while the right hand side is the distal. To capture the fast muscle contraction with a good temporal resolution, ultrasound plane wave imaging (5 MHz center frequency, 20 MHz sampling frequency) was used to scan the ROI and collect 2000 frames per second. A load cell (LC101-150, OMEGA Engineering, USA) was attached normally to the front of the shank to constrain the knee joint angle and record the force, F. The maximum joint torque during each contraction was computed and normalized based on F. The normalization first offsets force curve during each contraction to make the initial value zero and second divides all the results by the maximum of the first contraction after offsetting. The normalization removes the affects from the gravitational force, mg, inaccurate measurement of moment arm, sensor drifting, passive torque, τ_p, due to ligament or tendon, etc. Two electrodes (pads E) were placed along the thigh, through which the stimulator (Rehastim 1, HASOMED GmbH, Germany) sent pulse trains to stimulate the quadriceps muscle and produce the torque τ_a.

Experiment protocols: Experiment protocols were approved by the Institutional Review Board (IRB) of the University of Pittsburgh. A 24-year old able bodied male consented to participate in the experiments. The amplitude of each FES pulse train was 28 mA. The pulse frequency was 35 Hz. The pulse width was 300 μs. The fatiguing protocol starts with a 1 s for initialization of the experiment system and is followed by a 1.5 s FES pulse train to produce one muscle contraction every two seconds. There is a resting period of 0.5 s between consecutive pulse trains to let the muscle relax to the original position. The whole process lasts 81 s and there are 40 muscle contractions in total. Data synchronization is illustrated in Fig. 1b. Load cell measures the force at a 1 kHz sampling rate. Digital trigger signals are enabled every 8 s. They are sent as a 4 Hz pulse train with 0.8 % duty cycle to the ultrasound imaging system, which is configured to synchronously repeatedly fire all the 128 channels 500 times every time the rising edge of a trigger-in signal is detected. As a result, image data of 1 muscle contraction is recorded every 4 muscle contractions using ultrasound plane wave imaging. Consequently, image series of 10 muscle contractions along the whole fatigue process are collected. The subsequent analysis is based on the maximum normalized joint torque during each contraction and their synchronized image frames, from which the maximum strain images are computed.

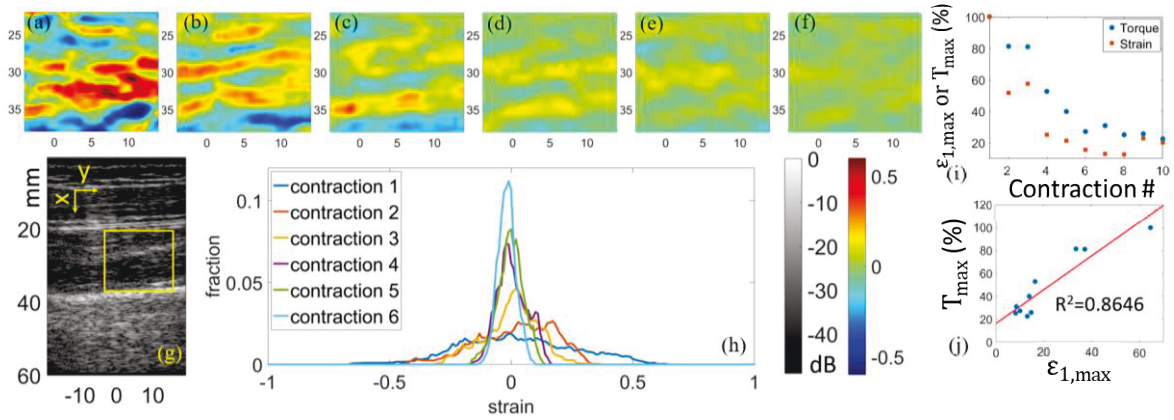

Figure 2: (a)-(f) Maximum axial strain images. (g) A B-mode ultrasound image of the quadriceps showing the ROI where the strain is computed. (h) Histograms corresponding to the maximum axial strain images. (i) The maximum torque and the maximum axial strain. (j) Correlation between the maximum normalized torque T_{max} and the maximum axial strain.

Results

Results are summarized by Fig. 2. The fatigue development is indicated by the maximum normalized joint torque during each of the 10 muscle contractions. The muscle is initially non-fatigued, namely in a pre-fatigue stage. In Fig. 2i, the strain data is further normalized to the maximum of the first muscle contraction so that both the torque and strain data start decreasing form 100 %. The decrease is noticeable along the first 6 contractions, namely a peri-fatigue stage. From the 6th to 10th contractions, the quadriceps muscle is close to a completely fatigued status, namely post-fatigue stage, and the torque does not have further obvious reduction. Corresponding to the torque during each of the first 6 muscle contractions, images of the maximum axial strain field are shown in Fig. 2, (a)-(f). Fig. 2h shows the histograms created from each of the maximum axial strain images. Fig. 2j presents the result of a linear regression between the maximum normalized joint torque and the maximum axial strain.

Discussion

Images of the maximum axial strain: The pattern of the strain field is consistent through the 1st contraction to the 6th contraction. The positive (red) strain represents for an extension while the negative (blue) strain represents for a compression along the axial direction. In this study on an axial strain field, the peak of the spatially distributed positive strain denotes a ROI of an active muscle contraction while the large negative strain is more likely a passive consequence of neighbourhood tissue interaction. For each image from Fig. 2a to Fig. 2f, two main positive axial strain peaks, which occur around the region $x = 26.0 \sim 35.0$ mm, $y = -4.0 \sim 14.0$ mm, indicate a region where the tissue deformation is a muscle contraction pattern. By comparing Fig. 2, (a)-(f), there is a noticeable reduction of positive strain peaks along the fatigue process. The maximum positive strain on each image, that is 0.646, 0.334, 0.371, 0.163, 0.139, 0.100, from the 1st contraction to the 6th contraction, show an overall decreasing trend. This fact indicates that the reduction of muscle deformation reflects contractility change during fatigue development and can be characterized by the axial strain field computed from ultrasound images. Moreover, the area of the positive axial strain can potentially be an additional evidence to indicate the fatigue process. By inspection on the maximum strain images with a proper threshold of 0.25, it is noted that the area approximated by counting pixels whose value is greater than 0.25 has an obvious reduction when muscle performs more and more contractions via FES. This suggests that fatigue not only gradually reduces the magnitude of muscle contraction but also incrementally suppresses the region where there is an active contraction pattern. Both effects were captured by the maximum axial strain images.

Correlated reduction of the maximum joint torque and the maximum axial strain: In Fig. 2i, for a better comparison, the strain data is further normalized to the maximum of the first muscle contraction so that both the torque and strain data start decreasing form 100 %. Both torque and strain curves delineate an exponential like trend by the data points 100 %, 81.4 %, 81.2 %, 52.8 %, 40.0 %, 27.2 %, 31.0 %, 25.2 %, 25.8 %, 22.5 % for torque and 100 %, 51.7 %, 57.5 %, 25.3 %, 21.5 %, 15.6 %, 13.2 %, 12.7 %, 22.8 %, 20.2 % for strain. This fact is consistent with the models discussed in [21], where FES-induced muscle fatigue shows characteristics of the first order dynamics. According to a common definition of muscle fatigue which is usually indicated by the degraded capability of producing maximum force, we investigated the correlation between the decreasing maximum strain (without normalization) and the torque during the fatigue process. In Fig. 2j, the linear regression result of $R^2 = 0.8646$ suggests a strong correlation and demonstrates the feasibility of using the derived strain field from ultrasound images to measure and monitor the whole transition period of fatigue development during FES operations. Further studies will be conducted across multiple human subjects to validate the result.

Implications from strain distributions: Histograms in Fig. 2h provide the distributions of the maximum axial strain field of the 6 muscle contractions during the peri-fatigue stage. Both the mean and median of each distribution except the 2nd contraction remains around 0. The variance decreases noticeably from the 1st contraction when

muscle is non-fatigued to the 6th contraction when muscle is completely fatigued. As a result, the probability density curve monotonically becomes sharper and sharper. The observation indicates a trend that, toward the post-fatigue stage, the maximum axial strain field becomes a more uniform map where most of the values concentrated around 0. This can be explained by the fact that muscle has both large positive and negative strain values when it is not fatigued because there not only exists a strong contraction stimulated by FES, but also exists a big tissue compression near a rigid boundary. For example, the large red area, $x = 30.0 \sim 35.0$ mm, in Fig. 2a is a noticeable contraction region while the blue area at a depth larger than 35.0 mm is a region close to the bone. However, when muscle is kept being stimulated by FES and gradually gets fatigued, the remaining weak contraction does not create the deformation of a great magnitude. The maximum axial strain field is therefore close to a uniform zero map.

Conclusion

The FES-induced fatigue development was assessed during a human isometric knee extension experiment using an ultrasound imaging-based methodology. The computed maximum axial strain images exhibit continued decrease of both overall magnitude and the total area of the large positive strain. The distributions of the maximum strain field vary towards a uniform zero strain map along the fatigue process. The fact that the reduction of the maximum axial strain strongly correlates with the reduction of the maximum joint torque suggests that the proposed methodology has a potential to stage the fatigue and is promising to help increase the effectiveness and accuracy of FES applications to restore limb functions of SCI patients.

Acknowledgement

This research was supported in part by the University of Pittsburgh Center for Research Computing through the resources provided.

References

[1] J. J. Abbas and H. J. Chizeck, "Feedback control of coronal plane hip angle in paraplegic subjects using functional neuromuscular stimulation," *IEEE Trans. Biomed. Eng.*, vol. 38, no. 7, pp. 687–698, 1991.

[2] C. L. Lynch and M. R. Popovic, "Functional electrical stimulation," *IEEE Control Syst.*, vol. 28, no. 2, pp. 40–50, 2008.

[3] N. Sharma, K. Stegath, et al., "Nonlinear neuromuscular electrical stimulation tracking control of a human limb," *IEEE Trans. Neural Syst. Rehabil. Eng.*, vol. 17, no. 6, pp. 576–584, 2009.

[4] R. J. Downey, T. H. Cheng, et al., "Switched tracking control of the lower limb during asynchronous neuromuscular electrical stimulation: theory and experiments," *IEEE Trans. Cybern.*, vol. 47, no. 5, pp. 1251–1262, 2017.

[5] N. Sharma, N. A. Kirsch, et al., "A non-linear control method to compensate for muscle fatigue during neuromuscular electrical stimulation," *Front. Robot. AI*, vol. 4, p. 68, 2017.

[6] C. S. Bickel, C. M. Gregory, et al., "Motor unit recruitment during neuromuscular electrical stimulation: a critical appraisal," *Eur. J. Appl. Physiol.*, vol. 111, no. 10, pp. 2399–2407, 2011.

[7] N. K. Vøllestad, "Measurement of human muscle fatigue," *J. Neurosci. Methods*, vol. 74, no. 2, pp. 219–227, 1997.

[8] G. C. Knowlton, R. L. Bennett, et al., "Electromyography of fatigue." *Arch. Phys. Med. Rehabil.*, vol. 32, no. 10, pp. 648–652, 1951.

[9] T. Sadoyama and H. Miyano, "Frequency analysis of surface EMG to evaluation of muscle fatigue," *Eur. J. Appl. Physiol. Occup. Physiol.*, vol. 47, no. 3, pp. 239–246, 1981.

[10] M. Cifrek, V. Medved, et al., "Surface EMG based muscle fatigue evaluation in biomechanics," *Clin. Biomech.*, vol. 24, no. 4, pp. 327–340, 2009.

[11] Y. Yoshitake, H. Ue, et al., "Assessment of lower-back muscle fatigue using electromyography, mechanomyography, and near-infrared spectroscopy," *Eur. J. Appl. Physiol.*, vol. 84, no. 3, pp. 174–179, 2001.

[12] M. Shinohara and K. Søgaard, "Mechanomyography for studying force fluctuations and muscle fatigue," *Exerc. Sport Sci. Rev.*, vol. 34, no. 2, pp. 59–64, 2006.

[13] M. O. Ibitoye, N. A. Hamzaid, et al., "Mechanomyography and muscle function assessment: A review of current state and prospects," *Clin. Biomech.*, vol. 29, no. 6, pp. 691–704, 2014.

[14] M. J. Dawson, D. Gadian, et al., "Muscular fatigue investigated by phosphorus nuclear magnetic resonance," *Nature*, vol. 274, no. 5674, pp. 861–866, 1978.

[15] F. Mandrile, D. Farina, et al., "Stimulation artifact in surface EMG signal: effect of the stimulation waveform, detection system, and current amplitude using hybrid stimulation technique," *IEEE Trans. Neural Syst. Rehabil. Eng.*, vol. 11, no. 4, pp. 407–415, 2003.

[16] D. Sierra González and C. Castellini, "A realistic implementation of ultrasound imaging as a human-machine interface for upper-limb amputees," *Front. Neurorobot.*, vol. 7, pp. 17:1–17:11, 2013.

[17] S. Sikdar, H. Rangwala, et al., "Novel method for predicting dexterous individual finger movements by imaging muscle activity using a wearable ultrasonic system," *IEEE Trans. Neural Syst. Rehabil. Eng.*, vol. 22, no. 1, pp. 69–76, 2014.

[18] R. S. Witte, K. Kim, et al., "Effect of fatigue on muscle elasticity in the human forearm using ultrasound strain imaging," in *Proc. IEEE Int. Conf. Eng. Med. Biol. Soc.*, 2006, pp. 4490–4493.

[19] J. Shi, Y.-P. Zheng, et al., "Assessment of muscle fatigue using sonomyography: muscle thickness change detected from ultrasound images," *Med. Eng. Phys.*, vol. 29, no. 4, pp. 472–479, 2007.

[20] M. A. Lubinski, S. Y. Emelianov, et al., "Speckle tracking methods for ultrasonic elasticity imaging using short-time correlation," *IEEE Trans. Ultrason. Ferroelectr. Freq. Control*, vol. 46, no. 1, pp. 82–96, 1999.

[21] R. Riener, J. Quintern, et al., "Biomechanical model of the human knee evaluated by neuromuscular stimulation," *J. Biomech.*, vol. 29, pp. 1157–1167, 1996.